

The dual klepsydra model of internal time representation and time reproduction

Jiří Wackermann^{a,*} and Werner Ehm^b

^a*Dept. of Empirical and Analytical Psychophysics*

^b*Dept. of Theory and Data Analysis*

Institute for Frontier Areas of Psychology, Wilhelmstrasse 3a, D-79098 Freiburg i. Br, Germany

Abstract

We present a model of the internal representation and reproduction of temporal durations, the ‘dual klepsydra’ model (DKM). Unlike most contemporary models operating on a ‘pacemaker-counter’ scheme, the DKM does not assume an oscillatory process as the internal time-base. It is based on irreversible, dissipative processes in inflow/outflow systems (‘leaky klepsydrae’), whose states are continuously compared; if their states are equal, durations are subjectively perceived as equal. Model-based predictions fit experimental time reproduction data with good accuracy, and show qualitative features not accounted for by other models. The deterministic model is characterised by two parameters, κ (outflow rate coefficient) and η (ratio of inflow rates). A stochastic version of the model (SDKM) assumes randomly fluctuating inflows, involves two more parameters, and accounts for intra-individual variance of reproduced durations. Analysis of the SDKM leads to non-trivial problems in the stochastic theory, briefly sketched here. Methods of parameter estimation for both deterministic and stochastic versions are given. Applying the DKM to the subjective experience of time passage, we show how subjective measure of elapsed time is constituted. Finally, essential features of the model and its possible neurophysiological interpretation are discussed.

Key words: Dual klepsydra model, Inflow/outflow systems, Internal time representation, Subjective experience, Time reproduction

* Corresponding author: J.W., Empirische und Analytische Psychophysik, Institut für Grenzgebiete der Psychologie, Wilhelmstrasse 3a, D-79098 Freiburg i. Br., Germany. Tel. +49 761 2072171. Fax +49 761 2072179.

Email address: jw@igpp.de (Jiří Wackermann).

1 Introduction

1.1 *Internal representation of temporal durations*

The importance of the time dimension for the understanding of functioning and behaviour of living systems is beyond any doubt. The characteristic times of biological processes range from 10^{-3} — 10^{-2} s (neural cells activity), over a broad range of periodic physiological activities (10^{-2} — 10^1 s) e. g., brain electrical oscillations, heart action, respiration, etc., to slow, ultradian, circadian, and infradian rhythms (10^4 s), studied by chronobiology (Aschoff, 1963; Scheving, Halberg, and Pauly, 1974; Winfree, 1980). The wide range of characteristic times, and the variety of physical and chemical processes involved, make hopes for a unitary theory of ‘biological’ or ‘physiological time’ (Carrel, 1931) rather unrealistic. There is also experimental evidence for different physiological mechanisms underlying perception of times in different orders of magnitudes, e. g. seconds vs. hours (Aschoff, 1998).

Of our interest is the domain in the order of magnitudes from few seconds to some tens of seconds, i. e., the domain in which temporal extension of an event is subjectively perceived as *duration*, and the intra-organismic representation of these durations. Shorter time intervals merge in a period of subjectively experienced ‘now’, a time window extending up to ≈ 2 — 3 s (Pöppel, 1978), while even shorter time intervals may lie below the order threshold ($\approx 10^{-1}$ s) or the fusion threshold ($\approx 10^{-2}$ s) (Atmanspacher and Filk, 2003). Longer time intervals, in the order of magnitudes of minutes and longer, are usually not perceived in a single perceptual act but rather fractioned and cognitively represented by means of interpolated temporal cues or conventional time units. Besides introspective evidence, objectively available physiological and behavioural data provide additional evidence for the relevance of the domain specified above, $\approx 10^0$ — 10^1 s. In the trace conditioning paradigm, conditioned reactions can be established with pairs of conditioned and unconditioned stimuli separated by periods of seconds or longer (Pavlov, 1927), although the strength of the conditioned reflex decreases with longer delays (Balsam, 1984). In complex, purposeful behaviour in animals, delayed reactions of relatively precise timing can be successfully entrained (Wing and Kristofferson, 1973; Church and Broadbent, 1990; Gibbon and Church, 1990) across a wide variety of species (Richelle and Lejeune, 1984).

These observations, in spite of their heterogeneous nature, demonstrate the ability of organisms to keep temporal information even in absence of an environmental *zeitgeber*, justify the hypothesis of *internal time representation*, presumably with a substrate in the central nervous system, and require a suitable biomathematical model of time representation.

1.2 Oscillatory time-base and the ‘internal clock model’

Early authors postulated a possible role of periodic physiological processes, e. g., heart action and respiration (Goudriaan, 1921), in intra-organismic time-keeping. Hoagland (1933) suggested rhythmic electrical activities of the neural system as a possible basis of internal time representation. Spontaneous brain electrical oscillations (electroencephalogram, EEG), particularly the α -rhythm with a characteristic frequency ≈ 10 Hz, were repeatedly suggested as the ‘physiological clock’ (Treisman, 1963; White, 1963; Holubář, 1969; Pöppel, 1972; Treisman, 1984). Experiments showed that external stimulation changing EEG frequency spectrum also affects the timing of conditioned physiological reactions (Holubář, 1969) or of behavioural responses (Wackermann and Miener, 2002).

Although the notion of a ‘physiological clock’ was keenly criticised by early proponents of cognitive psychology (Ornstein, 1969), the idea has been gradually adopted in the form of an abstract ‘internal clock model’ (ICM) (Church, 1984), which is now widely accepted as the ‘standard’ model of internal time representation (Block, 1990; Treisman et al., 1990; Zakay and Block, 1997; Grondin, 2001; Wearden, 2004). The model (Fig. 1) consists of a pulse generator, or ‘pacemaker’ P , emitting discrete pulses at a constant frequency f_P . Its output is directed through a gate, or ‘switch’ S , controlled by environmental events E , to an accumulator A . The pulse count is stored in a ‘working memory’ M_w , from where it can be further transferred to a long-term, ‘reference memory’ M_r . The states of the memory registers M_w and M_r are compared in the comparator C , output of which is translated to a behavioural response.

Figure 1 about here.

The ICM is essentially an abstraction of a simple stop-watch, in which the ticks of a periodic pacemaker are counted, the momentary count is displayed as a position of the pointer (M_w), and eventually matched by a human observer (C) against marks imprinted on the clock face (M_r). Thus, the model is determined by our culture’s time measurement technology, which is based on regular oscillatory processes since Huygens’ (1673) invention of the pendulum-driven clock. However, the history of chronometry (Janich, 1980; Whittrow, 1988) shows that ‘tick counting’ is only one among many possible construction principles. Time-keeping devices of early cultures were based rather on irreversible transformations of matter or energy—e. g., burning candles or oil lamps, or leaky water containers, *klepsydrae*¹. Irreversible, energy-dissipating processes are also characteristic for the realm of living systems (e. g. metabolic degradation of organic molecules, relaxation of excited neural cell, etc.), far more than reversible, energy-preserving harmonic oscillations (e. g., swinging pendulum). Timing mechanisms based on such irreversible processes may provide metaphors or models more adequate to biological reality than mechanical tick-counter models.

¹ Greek $\kappa\lambda\epsilon\psi\upsilon\delta\rho\alpha$ = water-clock, derived from $\kappa\lambda\epsilon\pi\tau\omega$ = steal and $\upsilon\delta\omega\rho$ = water.

1.3 The problem of time reproduction

Among numerous experimental methods used in studies of human time perception (Woodrow, 1951; Bindra and Waksberg, 1956), the methods of *time production* and *time reproduction* are of special interest for our purpose. In a ‘time production task’ (TPT), a duration is given in numeric form, e. g., “10 seconds”, and the subject is instructed to mark a time interval of the given duration by a motor or verbal action. In a ‘time reproduction task’ (TRT), a sensory stimulus² —e. g., an audible tone or a visual object shown on a screen—is given, and the subject has to reproduce its duration by a motor action—e. g., pressing two times a switch which starts/stops the sound, or displays/conceals the visual target. In experiments with a precisely controlled inter-stimulus interval (ISI), the onset of the reproduction period is determined by the experimental schedule, and the subject is requested only to mark the end of the reproduced interval.³

Variations in TPT data are apparently easy to interpret in terms of the ICM: A subject, asked to produce the same duration, s , in two experimental conditions, may produce duration r_1 in condition 1 and r_2 in condition 2. According to the ICM the accumulated pulse counts should be the same,

$$r_1 f_{P,1} = r_2 f_{P,2}, \quad (1)$$

so $r_1 \neq r_2$ implies $f_{P,1} \neq f_{P,2}$, and so the common interpretation is that the pacemaker’s frequency differs between conditions (e. g. Koch et al. (2003)).

Interpretation of TRT data in terms of the ICM meets difficulties. If the pacemaker keeps a constant frequency f_P during a (relatively short) TRT trial, the reproduced duration r should be exactly equal⁴ to the presented duration s . However, experimental data show that the average reproduced times are usually significantly *shorter* than the presented time s (Fig. 2a). A possible interpretation is that the pacemaker frequency during the r -phase was higher compared to the s -phase of the TRT trial, $f_{P,r} > f_{P,s}$. The reproduced times then should be *proportionally* shortened by factor $f_{P,s}/f_{P,r}$ in order to preserve equality (1). This is not the case, as can be seen from

² To avoid terminological difficulties, we will deviate from the usual nomenclature of experimental psychology. In the following we denote the sensorily perceivable stimuli, used to mark the time intervals, as ‘carriers’ of their respective durations. For the sake of brevity, we call presentation of the carrier of the duration to be reproduced an ‘ s -phase’, and presentation of the carrier of the reproduced duration an ‘ r -phase’.

³ Since TRT does not refer to culturally imprinted time standards or units, it is a preferable method to study biological background of time perception. Inversely, timing of foraging activities (Richelle and Lejeune, 1984) or of conditioned responses (Holubář, 1969) may be considered as a special kind of behavioural reproduction of entrained time intervals.

⁴ Up to an uncertainty in the order of magnitude of f_P^{-1} , due to the discrete nature of the ‘internal clock’.

the course of average reproduced durations plotted as a function of presented durations, varied over a broad time range (empirical time reproduction curves, TRCs). Fig. 2b shows two such TRCs obtained by A. Eisler (2003)⁵ for two ethnic populations. In both groups the reproduced times were not only systematically shorter, but showed even *progressive* relative shortening, as indicated by the negative curvature of the TRCs, and obvious from the roughly linear decrease of ratios r/s plotted against presented durations s (Fig. 2b, top).

Figure 2 about here.

Another problem arises from comparisons of TPT and TRT data. For example, Pöppel and Giedke (1970, p. 193, Fig. 7) found parallel variations of produced (TPT of 10 s intervals) and reproduced times (TRT of 6 s intervals) in the diurnal cycle, which are difficult to explain in terms of the ICM. It is well conceivable that the pacemaker rate f_P exhibits slow circadian variations, but it is unclear why such variations should be reflected by the TRT data.

In summary, the ICM postulating a constant (or only slowly fluctuating) pacemaker rate cannot account for the above-mentioned phenomena observed in TRT data; and a model with a variable pacemaker rate would have to comprise a mechanism controlling the clock rate to account for the TRT data, but no such extended model has been proposed so far. As recently pointed out by Wearden (2004, pp. 314–315),

“some other timing procedures [...] used in classical time psychology such as reproduction and verbal estimation not only may not have any clear theoretical model which accounts for them, but may also be resistant to simple models of the sort” [i. e., ICM].

2 Dual klepsydra model of time reproduction

2.1 Inflow/outflow systems as time-keepers

Any system whose state changes as a monotonic function of physical time t can, in principle, serve as a time-keeping device. Such a system need not reproduce the structure of an ordinary ‘ticking’ clock: counting is but a special case of integration. A water-clock accumulating water flowing in at a constant rate may serve as an example of an integrator with a continuous state variable. Mechanical or electronic tick counters, non-leaking containers, etc., preserve their states for infinite time; a kind of reset mechanism is required to re-use such loss-less integrators for time-keeping. However, ‘lossy’, passively relaxing systems—e. g. the ancient

⁵ Original data were not available. For the purpose of the present paper, data were scanned and digitised from a magnified copy of Fig. 3 in (A. Eisler, 2003, p. 14).

Greek *klepsydrae* mentioned in section 1.2—, showing monotonic state change with time may serve as time-keeping devices as well. They operate within a finite time horizon, but they do not require any special reset mechanism.

Figure 3 about here.

Of our interest are *inflow/outflow systems* (IOSS) combining both principles, integration of an external input, and spontaneously occurring relaxation. Generally, IOSS display two essential features: monotonic increase of the state variable up to a steady-state equilibrium, determined by internal properties of the IOS *and* the intensity of the input; and a passive return to the base state in absence of external input. A ‘leaky water-clock’ (Fig. 3a) is an example of such an IOS; analysis of hydrodynamic IOSS gives a good introduction into a study of IOSS and their properties in general (Appendix A). In this paper we study time-keeping systems composed of linear IOS, described by the differential equation

$$dy = (i - \kappa y) dt, \tag{2}$$

e. g., a capacitor-resistor circuit with $\kappa = (RC)^{-1}$, fed by electric current of constant intensity i , and accumulating charge y on the capacitor C (Fig. 3b). Eq. (2) is solved by

$$y_t = y_0 e^{-\kappa t} + \bar{y} (1 - e^{-\kappa t}), \tag{3}$$

where y_0 is the initial state at $t = 0$, and $\bar{y} \equiv \lim_{t \rightarrow \infty} y_t = i/\kappa$ is the steady-state equilibrium. Hereinafter we also refer to these systems as ‘klepsydrae’, although their equations naturally differ from those of hydrodynamic IOSS.⁶

2.2 Dual klepsydra model of time reproduction: constant inflows

Consider a system consisting of two ‘klepsydrae’, 1 and 2, and a time reproduction task (TRT) with stimulus duration s and inter-stimulus time w (Fig. 4a). Klepsydra 1 starts at state $y_{1,0} = 0$, is being filled with inflow i_1 up to time $t = s$, and leaking with decrement κ afterwards. Klepsydra 2 starts at the beginning of the reproduction phase at state $y_{2,s+w} = 0$ and is being filled with inflow i_2 (in general, $i_1 \neq i_2$).

Figure 4 about here.

⁶ Hellström (1998) proposed an abstract psychological model of subjective time in which ‘mental content flow’ is accumulated on a similar principle. His formalism as well as the nature of hypothetical ‘mental content’ are unclear.

We assume that the presented and reproduced durations are subjectively perceived as equal when the states of the two klepsydrae become equal, $y_{1,t} = y_{2,t}$, at time $t = s + w + r$. This leads to the equation

$$\bar{y}_1 (1 - e^{-\kappa s}) e^{-\kappa w} e^{-\kappa r} = \bar{y}_2 (1 - e^{-\kappa r}), \quad (4)$$

where $\bar{y}_j \equiv i_j/\kappa$ are the limiting states for klepsydrae $j = 1, 2$; let $\eta \equiv \bar{y}_1/\bar{y}_2 = i_1/i_2$ denote their ratio. From eq. (4) follows

$$e^{\kappa r} = 1 + \eta e^{-\kappa w} (1 - e^{-\kappa s}) \quad (5)$$

and thus

$$r = \kappa^{-1} \log \left(1 + \eta e^{-\kappa w} (1 - e^{-\kappa s}) \right). \quad (6)$$

Considering r as a function of the presented duration s and the inter-stimulus interval $w \geq 0$, we define the *klepsydra reproduction function* (KRF),

$$r(s|w) = \kappa^{-1} \log \left(1 + \eta e^{-\kappa w} (1 - e^{-\kappa s}) \right), \quad (7)$$

with parameters $\kappa > 0$ (leakage) and $\eta > 0$ (infbw ratio). The form of the KRF is determined by the term $\eta_* \equiv \eta e^{-\kappa w}$ (reduced infbw ratio). It starts at $r(0|w) = 0$, with a slope η_* , and is monotonically increasing, approaching asymptotically the limit $\kappa^{-1} \log(1 + \eta_*)$ for $s \rightarrow \infty$.⁷

In most TRTs physical carriers with the same physical properties are used (e. g., empty or homogeneously filled time intervals) to mark the presented/reproduced durations; we then assume equal infbws, $i_1 = i_2$, and thus $\eta = 1$. In this ‘normal case’, the reduced infbw ratio is always $\eta_* \leq 1$ (with equality for a vanishing inter-stimulus interval $w = 0$), and the entire KRF is then located below the line of exact reproduction $r = s$ (Fig. 5a).

The dual klepsydra model (DKM) thus naturally accounts for both phenomena observed in empirical TRCs (section 1.3): (i) the consistent under-reproduction of time intervals, and (ii) the progressive shortening of reproduced times, manifested by the negative curvature of the theoretical TRC. The question of how to interpret the model parameters κ and η will be addressed in the concluding section 3.

Figure 5 about here.

⁷ The derivative of the KRF w.r.t. its first argument can be written as $\partial_s r(s|w) = \eta e^{-\kappa(s+w+r)}$, where the quantities t , w , and r appear in the argument of the exp function as their algebraic sum, i. e., as additive parts of the same continuum. This motivates our study of reproduction of partitioned time intervals in section 2.5.

2.3 Dual klepsydra model of time reproduction: stochastic inflows

The DKM proposed in the preceding section is a deterministic model, based on ordinary differential equations and yielding a unique value of the response r to a stimulus s . However, experimental data show a considerable variance of responses for each given stimulus duration s (Fig. 2a). A realistic model should account for the response variability as an *intrinsic* feature of the reproduction process. In this section we briefly outline a stochastic version of the model (SDKM).

We assume that infbws i are not constant but randomly fluctuating with dispersion σ ; eq. (2) then becomes a stochastic differential equation (Karatzas and Shreve, 1991),

$$dY_t = (i - \kappa Y_t) dt + \sigma dW_t, \quad (8)$$

where W_t is the standard Wiener process scaled by σ . The solution to eq. (8) is

$$Y_t = y_0 e^{-\kappa t} + \bar{y} (1 - e^{-\kappa t}) + \sigma U_t,$$

where y_0 is the initial state, $\bar{y} \equiv i/\kappa$ as in section 2.1, and

$$U_t = \int_0^t e^{-\kappa(t-\tau)} dW_\tau$$

is the Uhlenbeck-Ornstein (1935) process.

The dual klepsydra scenario is the same as given in the preceding section (Fig. 4b). Klepsydra 1 is filled with infbw i_1 during the time interval s up to a state $Y_{1,s}$, which is now a random variable, and then leaks. Klepsydra 2 starts at state $Y_{2,s+w} = 0$ and is filled with infbw i_2 , until its state matches the state of the leaking klepsydra 1. The first passage time determines the response in the reproduction task,

$$R = \inf \left\{ r \geq 0 : Y_{2,s+w+r} = Y_{1,s} e^{-\kappa w} e^{-\kappa r} \right\}, \quad (9)$$

which is a random variable. Its distribution, the *klepsydra reproduction distribution* (KRD) \mathcal{R} , depends on the stimulus duration s , the waiting time w , and the SDKM parameters $\kappa, i_1, i_2, \sigma_1, \sigma_2$ characterising klepsydrae 1 and 2. The times s and (usually) w are determined by the experimental design; the SDKM parameters are unknown and have to be estimated from the data.

This task requires the determination, or at least some partial knowledge, of the KRD. In principle, this distribution can be determined exactly, i. e., its Laplace transform

can be derived in explicit form (Ehm and Wackermann, 2003). However, the analytic complexity of the resulting expression limits its practical use. Therefore we resort to a stochastic approximation to the random variable R that yields accurate approximations for the first two moments of R and suggests a roughly normal shape of \mathcal{R} (Appendix B). The approximations $m \approx \langle R \rangle$ and $v \approx \text{var } R$ to the exact mean and variance of R are

$$m = \kappa^{-1} \log \xi \quad (10)$$

and

$$v = (2\kappa)^{-1} \gamma_2^{-2} \xi^{-2} \left(\xi^2 - 1 + \rho^2 e^{-2\kappa w} (1 - e^{-2\kappa s}) \right), \quad (11)$$

where, in addition to $\eta \equiv i_1/i_2$, we abbreviate $\gamma_j \equiv i_j/\sigma_j$ ($j = 1, 2$), $\rho \equiv \sigma_1/\sigma_2$, and $\xi \equiv 1 + \eta e^{-\kappa w} (1 - e^{-\kappa s})$.

Note that the approximate mean of the KRD equals the value of the KRF for given s , $m = r(s|w)$, and thus involves only the DKM-parameters κ, η , whereas the approximate variance v depends additionally on the *noise ratio*, ρ , and on the *signal-to-noise ratio*, γ_2 , of klepsydra 2.⁸ The exact Laplace transform of \mathcal{R} , hence \mathcal{R} itself, depends on the same set of four parameters; so at least in this respect there is no information loss when using the normal distribution $\mathcal{N}(m, v)$ as a working approximation to \mathcal{R} (see below, section 2.4.2).

2.4 Estimating DKM parameters

The task is to estimate the model parameters, κ and/or η , from experimental data consisting of N triples (s_n, w_n, r_n) where s_n is the presented duration, w_n is the ISI, and r_n is the reproduced duration in the n th trial ($n = 1, \dots, N$). As will be shown in the following, simultaneous estimates of both parameters are strongly correlated, but often we are interested in two types of tasks: (i) estimate κ from data obtained with homogeneous duration carriers, i. e., with fixed value $\eta = 1$; or (ii) estimate η for inhomogeneous carriers, with a value of κ estimated from data with homogeneous carriers.

2.4.1 Deterministic model

The deterministic version of the model (section 2.2) predicts only expected values of reproduced times and, unlike the stochastic model, does not account for the intra-

⁸ The parametrisation is merely a matter of convention. Given η and ρ , γ_1 could be used instead of γ_2 since the four parameters are bound by the relation $\gamma_1/\gamma_2 = \eta/\rho$.

individual variance. Assuming a simple additive error model, we use the method of weighted least squares (WLSQ), minimising the error criterion

$$S = \sum_n g(s_n) (r_n - r(s_n|w_n))^2, \quad (12)$$

where (s_n, r_n) are the presented/reproduced durations, w_n are the ISIs, $r(\cdot|\cdot)$ is the KRF (eq. 7), and $g(\cdot)$ is a suitably chosen weight function. In practice we choose $g(t) = t^{-1}$ to compensate for the increase of variance of the reproduced times with increasing duration s (Woodrow, 1930). The method can also be applied to reproduced times averaged across repeated presentations of the same s . The partial derivatives of criterion S w. r. t. model parameters do not yield ‘normal equations’ from which the parameters could be directly calculated; an iterative procedure is required to determine exactly the minimum of the criterion S . (A method for an approximative but direct estimate of κ is given in Appendix C.)

For a data subset from a TRT study by Wackermann and Miener (2002) shown in Fig. 2 the WLSQ estimate is $\hat{\kappa} = 7.5 \times 10^{-3} \text{ s}^{-1}$. For TRT data published by A. Eisler (2003) we find $\hat{\kappa} = 1.7 \times 10^{-2} \text{ s}^{-1}$ for the Swedish population and $\hat{\kappa} = 3.3 \times 10^{-2} \text{ s}^{-1}$ for the African population. In spite of different methods and stimulus ranges used in different studies, these estimates are in good agreement as to their order of magnitudes, and the theoretical TRCs generated by eq. (7) fit the data with good accuracy (cf. Fig. 5ba, 5bb).

2.4.2 Stochastic model

Let (s_n, w_n, r_n) ($n = 1, \dots, N$) be experimental data as in the preceding section. The reproduced durations r_n are here considered as (stochastically independent) random variables with distributions \mathcal{R}_n as specified by the SDKM. These KRDS are well approximated by normal distributions $\mathcal{N}(m_n, v_n)$, where m_n, v_n are given by eqs. (10), with data s_n and w_n substituted for s and w . A straightforward approach is to minimise the negative Gaussian log-likelihood,

$$L \equiv L(\kappa, \eta, \gamma_2, \rho) = \frac{1}{2} \sum_n \left(\frac{(m_n - r_n)^2}{v_n} + \log v_n \right), \quad (13)$$

simultaneously over all four parameters, on which L depends via the quantities m_n and v_n . However, this approach fails: due to the particular nonlinear dependency of the quantities v_n on the parameters, the resulting estimates are generally grossly biased and tend to attain values at the boundary of the parameter space. A viable alternative is to proceed stepwise: (i) estimate the primarily important parameters κ and η , using WLSQ as above, and (ii) using the estimates $\hat{\kappa}, \hat{\eta}$, obtained in step (i), apply the quasi log-likelihood procedure (13) to estimate the other two parameters. Technical details and results of a simulation study are given in Appendix B.

2.5 DKM and the measure of subjective time passage

Analysis of certain properties of the DKM and its reproduction function may also provide interesting insights into the nature of the subjective experience of time passage (Wackermann, 2004). Of interest is now subjective measure of time elapsed. For the rest of this section, we assume physically homogeneous carriers of given intervals, thus $\eta = 1$.⁹

Figure 6 about here.

Consider a time interval of duration $s > 0$, divided into two subintervals of durations t_1 and t_2 , $t_1 + t_2 = s$ (Fig. 6). It can be easily shown that

$$r(t_1|t_2) + r(t_2|r(t_1|t_2)) = r(t_1 + t_2|0). \quad (14)$$

This can be applied to further division of any of the subintervals, etc.; we thus arrive at a rule of *serial additivity of reproduced times* for the KRF:

Let $s > 0$ be a given duration subdivided into $N > 1$ intervals of durations t_n (such that $t_1 + \dots + t_N = s$), and $w \geq 0$ a waiting time. Let r_n denote the partial reproduction of the n -th interval, ($n = 1, \dots, N$), and u_n denote the delay between the end of the n -th interval and the beginning of its reproduction,

$$r_n = r(t_n|u_n), \quad u_n = \sum_{\nu=n+1}^N t_\nu + w + \sum_{\nu=1}^{n-1} r_\nu.$$

Then the sum of partial reproductions equals the reproduction of the total duration, i. e.,

$$\sum_{n=1}^N r(t_n|u_n) = r(s|w).$$

In our conceptualisation, the fact that elapsed duration is internally represented is manifested by the subjects' ability to re-produce *at present* the temporal moments of the *past*. Consider a time interval of fixed duration s , and a sequence of 'past nows',

$$0 \leq t_1 < t_2 < \dots \leq s;$$

⁹ Even in absence of specific 'carriers' marking the elapsed durations, the permanent stream of proprioceptive sensations may be the source of constant inflows for the klepsydrae.

this is mapped to the sequence

$$0 \leq r(t_1|s - t_1) < r(t_2|s - t_2) < \dots \leq r(s|0).$$

Properties of this mapping can be studied by means of the *cumulative reproduction function*, defined for $t \in [0; s]$ (where s is given and fixed) as

$$\mathcal{T}(t) \equiv r(t|s - t) = \kappa^{-1} \log \left(1 + e^{-\kappa s} (e^{\kappa t} - 1) \right), \quad (15)$$

The derivative of function \mathcal{T} w.r.t. physical time t ,

$$\rho \equiv \frac{d\mathcal{T}}{dt} = e^{-\kappa(s-t+\mathcal{T})}, \quad (16)$$

may be considered as the ‘density’ of the subjective time flow; it is a positive and *increasing* function of physical time t (Fig. 7). The mapping of the past ‘nows’ to present (reproduced) ‘nows’ is thus monotonic (preserving time order) but non-linear. The recent past has more weight than the more distant past¹⁰, or, phrased in the language of subjective introspection, “time flows with an increasing speed”.

Figure 7 about here.

3 Discussion and conclusions

The ‘dual klepsydra model’ (DKM), presented in the preceding sections, shares with the commonly accepted ‘internal clock model’ (ICM; section 1.2) the notion of an integration of a ‘flow’: a stream of discrete pulses in the ICM, or a continuous flow in the DKM. However, the two models essentially differ in the following features:

(i) *The concept of an integrator*: Unlike the ‘pulse counters’ in the ICM, the accumulators in the DKM are inflow/outflow systems of the ‘leaky klepsydra’ prototype, i.e., passively losing their accumulated state in absence of external input.¹¹ The basic building elements are thus formally similar to the ‘leaky integrate-and-fire’

¹⁰ This is in agreement with Allan’s (2002) findings from experiments with time intervals bisection, while the ‘mental content flow’ model proposed by Hellström (1998) predicts exactly the opposite, i.e., faster ‘flow’ at the beginning of the remembered/reproduced interval.

¹¹ In the limiting case $\kappa = 0$, the DKM becomes functionally equivalent to the ICM, with the inflow ratio $\eta \equiv i_1/i_2$ formally replacing the ratio of pacemaker frequencies during the presentation and reproduction phase, $f_{P,s}/f_{P,r}$. However, $\kappa > 0$ is required to fit empirical TRT data, as shown in sections 1.3 and 2.4.

neuron, a standard computational model for neural populations (Tuckwell, 1988; Gerstner, 2002), but they cannot be identified with single neurons, operating on entirely different time scales (see below). Leaky accumulators fed with stochastic input have also been used in mathematical psychology to model perceptual and decision processes (Usher and McClelland, 2001).

(ii) *The status of time cognition*: The fusion of the notion of ‘physiological clock’, operating on an oscillatory basis, with the notion of ‘subjective’ or ‘psychological’ time has resulted in a conceptual confusion: the states of ‘memory registers’, ‘pulse counters’, i. e., the ‘readings’ of the ‘internal clock’, are commonly identified with the ‘internal time’ data.¹² By contrast, in our concept the states of the accumulators (‘klepsydrae’) are inaccessible to direct observation; only results of state comparisons provide *hints* necessary for the constitution of the subjective measure of elapsed time (section 2.5). We therefore conceptualise time reproduction as a ‘proto-cognitive’ (also ‘ur-cognitive’: Wackermann (2004)) operation, out of which the cognitive constructs arise.¹³

In an earlier paper (Wackermann, Ehm, and Späti, 2003) we have proposed an interpretation of the ‘klepsydrae’ as circumscribed neural assemblies, accumulating excitation caused by internal processing of the carrier stimuli (‘neural flows’), and then relaxing to their base state. The expression ‘relaxation’ insinuates a passive process, but processes of active inhibition may play a role, too. According to this hypothesis, the ratio η would be predominantly determined by the properties of the environmental (sensory) input, while the de-excitation component of the process would be determined by the functional state of the neural substrate. The DKM conceptually separates but functionally combines these two aspects of alleged neural processes underlying internal time representation: η stands for the exogenous, κ for the endogenous, organismic component of the process. Consequently, we hypothesise that κ should reflect the dependence of time perception on global organismic state variables, e. g., temperature (Hoagland, 1933; Pfaff, 1968; Wearden and Penton-Voak, 1995), vigilance (Wackermann et al., 2002), etc. Variations of physical properties of the environmental input (‘carriers’) and/or of its information content (Ornstein, 1969) may affect time perception via the infbw ratio η .

The system-proper internal time scale is obviously determined by the ‘leakage’ component, represented by the parameter κ . This relates our model to earlier theories of time representation, postulating neural trace decay as a basis of time judgment (James, 1890, vol. 1, chapter 15). The estimates of the parameter κ from available TRT data were in the range

¹² This applies also to the ‘parallel-clock model’ proposed by H. Eisler (1975). Eisler’s model also consists of two sub-units, states of which are continuously compared, but basic premises of his approach are very different from ours.

¹³ Discussion of relations between our concept of reproduction as a primitive operation preceding metric constructs, and fundamental issues in the theory of time measurement (Reichenbach, 1957) would drift too far away from the present topics. For a discussion of our results in an interdisciplinary context see (Wackermann, 2005).

≈ 0.75 to $3 \times 10^{-2} \text{ s}^{-1}$ (see section 2.4.1). Their inverse, κ^{-1} , provides estimates of relaxation times of the hypothetical IOSs ('neural klepsydrae'), which are in the range from half-minute (African population) to about two minutes (German population). These values are by about 3–4 orders of magnitude larger than time constants of single neural cells (Kandel, Schwartz, and Jessell, 2000). However, comparable time constants can be found on higher levels of neural integration, e. g., in sensory subsystems, or even the brain as a whole. For example, longest decay times of figural after-effects following sensory stimulation are ≈ 100 – 150 s (Oyama, 1978). Brain electrical data may provide more direct evidence into time scales of the global brain dynamics: decay times of EEG auto-correlation functions are reported in the range $\approx 100 \text{ s}$ (Linkenkaer-Hansen et al., 2001). Specific experiments will be required to decide if this is merely a coincidence or whether this agreement in the order of magnitudes of $\approx 10^2 \text{ s}$ indicates a real relationship between internal time representation and the long-term temporal binding detectable in brain electrical activity.

The neurobiological implementation of the DKM is here proposed in terms of general properties of excitable neural tissues, and in entirely functional terms. There is an increasing body of clinical observations (von Steinbüchel, Wittmann, and Szélag, 1999; Koch et al., 2002; Pouthas and Perbal, 2004), experimental findings (Koch et al., 2003), and cumulative knowledge on neuroanatomical structures (Rubia and Smith, 2004) or neurochemical mechanisms (Rammsayer, 1990, 1992) involved in time perception; but only systematic and model-based experimental work may bring order to the bulk of empirical findings. At the present state of knowledge we abstain from making hypotheses about possible cerebral localisation and/or structural identification of the underlying neural mechanisms.

While the DKM appears to be superior to the ICM regarding the interpretation of TRT data, interpretation of data obtained with different experimental methods remains a challenge. The next domain of application could be *duration discrimination* in pairwise comparisons of sequentially presented time intervals, and explanation of effects like 'time order error' (TOE) (Woodrow, 1951; Allan's, 2002; Hellström, 2003), i. e., dependence of the response tendency on the order of presentation of stimuli. Wearden and Ferrara (1993) proposed the possibility of a change of memory representation of temporal durations with progressing time to explain the TOE, but this proposal was not further developed to a specific, quantitative model. The DKM seems to be particularly suitable for this purpose, because here memory 'loss' is not a *post hoc* correction but an *ex ante* assumption.

Acknowledgements

The authors wish to thank Harald Atmanspacher and Stefan Rotter for helpful comments on an earlier draft of the paper; Simon Grondin and Åke Hellström for kindly providing copies of otherwise unavailable papers; and Matthias Gäßler and Jakub Späti for technical assistance.

A Brief review of hydrodynamic inflow/outflow systems

A simple hydrodynamic IOS, the ‘leaky klepsydra’, is a cylindric container of cross-section area A , with an opening of cross-section area $B \ll A$ at its bottom (Fig. 3a), filled at a constant inflow rate, $I = dV/dt \geq 0$. Let y denote the height of the accumulated liquid, g be acceleration due to gravity, and $i \equiv \frac{I}{A}$, $k \equiv \frac{B}{A}\sqrt{2g}$. The system is described by the differential equation

$$dy = (i - k\sqrt{y}) dt, \quad (\text{A.1})$$

which is solved by

$$\sqrt{y_t} - \sqrt{y_0} + \sqrt{\bar{y}} \log \frac{\sqrt{\bar{y}} - \sqrt{y_t}}{\sqrt{\bar{y}} - \sqrt{y_0}} = -\frac{1}{2}kt, \quad (\text{A.2})$$

where y_0 is the initial state and $\bar{y} \equiv (i/k)^2$ is the steady-state equilibrium. In the special case $y_0 = 0$, eq. (A.2) simplifies to

$$\sqrt{y_t} + \sqrt{\bar{y}} \log \left(1 - \frac{\sqrt{y_t}}{\sqrt{\bar{y}}} \right) = -\frac{1}{2}kt.$$

In the outflow-only case ($i = 0$), eq. (A.2) simplifies to

$$\sqrt{y_t} - \sqrt{y_0} = -\frac{1}{2}kt,$$

in which case the state y can be expressed explicitly as a function of t ,

$$y_t = \begin{cases} \left(\sqrt{y_0} - \frac{1}{2}kt \right)^2 & \text{for } 0 \leq t \leq t_e \\ 0 & \text{for } t_e < t \end{cases}, \quad (\text{A.3})$$

where $t_e \equiv 2k^{-1}\sqrt{y_0}$ is the outflow time.

Physically interesting are also ‘leaky klepsydrae’ with shaped containers, where the cross-section area $A(y)$ varies as a function of height y . Consider, for example, $A(y) = \bar{A}S(y)$, with the average cross-section area \bar{A} and the ‘shape function’ $S(y) = cy^\alpha$ determined by the exponent α . This class of IOSs, including the cylindric klepsydra as a special case ($\alpha = 0$), is described by the differential equation of the form

$$dy = \left(iy^{-\alpha} - ky^{1/2-\alpha} \right) dt,$$

where $i \equiv \frac{I}{A}$ and $k \equiv \frac{B}{cA}\sqrt{2g}$. In the outflow-only case ($i = 0$), all these IOSs show finite outflow times, except of the hyperbolic klepsydra $\alpha = -\frac{1}{2}$, leaking out exponentially,

$y_t = y_0 e^{-kt}$. In presence of inflow, $i > 0$, however, this system is *not* equivalent to the linear IOS treated in section 2.1.

B Stochastic approximation of the KRD

A stochastic approximation to the first passage time R (section 2.3, eq. 9) is derived as follows. In the equation defining R ,

$$\gamma_2 (1 - e^{-\kappa R}) + \sigma_2 U_{2,R} = Y_{1,s} e^{-\kappa w} e^{-\kappa R}, \quad (\text{B.1})$$

(i) set $R = r + \Delta$, where $r \equiv r(s|w)$ is the value of the KRF for stimulus duration s , i. e., the matching time of the two deterministic klepsydrae, and Δ is a random deviation. Supposing Δ small, (ii) approximate $U_{2,R} \approx U_{2,r}$ in eq. (B.1), and (iii) solve the resulting equation for R . This gives the approximation

$$R \approx \kappa^{-1} \log \frac{\gamma_2 + Y_{1,s} e^{-\kappa w}}{\gamma_2 + \sigma_2 U_{2,r}}.$$

Finally, (iv) using Taylor expansion $\log(1+x) \approx x$ and inserting the explicit expression for $Y_{1,s}$ gives

$$R \approx r + \frac{1}{\gamma_2} \left(\frac{\rho}{\xi} e^{-\kappa w} U_{1,s} - U_{2,r} \right). \quad (\text{B.2})$$

The r. h. s. of (B.2) represents a stochastic approximation to R that is linear in the two independent Gaussian random variables $U_{1,s}$, $U_{2,r}$, hence is itself normally distributed. The mean m and variance v of the linear combination are easily calculated, with the result given in (10).

The stochastic approximation and the ensuing normal approximation should be satisfactory if the signal-to-noise ratios of the klepsydra processes, $\gamma_{1,2}$, are sufficiently large. The mean and variance approximations are in fact fairly good for signal-to-noise ratios down to 1, and excellent for $\gamma_{1,2} \geq 3$, across a broad range of parameter values of interest. The shape of the exact distribution \mathcal{R} is by and large Gaussian with some skewness to the right depending primarily on the signal-to-noise ratios $\gamma_{1,2}$ and the value of κ .

C Approximate estimation of parameter κ

Of prime interest are estimates of the parameter κ , while the value of parameter η is fixed. The weighted least squares (WLSQ) method proposed in section 2.4.1 requires an iterative numeric procedure to find $\hat{\kappa}$ minimising the error criterion S . An approximate but direct

method to estimate κ is as follows. Considering the reproduced time, r , given by eq. (6) as a function of κ , and taking the first three terms of its Taylor expansion at $\kappa = 0$, we have a quadratic (in κ) approximation to r ,

$$\begin{aligned} \tilde{r}(s|w) = \eta s & \left[1 - \kappa \left(s \frac{1+\eta}{2} + w \right) \right. \\ & \left. + \kappa^2 \left[s^2 \left(\frac{\eta^2}{3} + \frac{\eta}{2} + \frac{1}{6} \right) + sw \left(\frac{1}{2} + \eta \right) + \frac{w^2}{2} \right] \right] \end{aligned} \quad (\text{C.1})$$

Using the approximation $\langle r_n \rangle \approx \tilde{r}(s_n|w)$ for the expectations of the random reproduced times r_n and summing over n gives, after division by $\eta \sum_n s_n$, the approximate identity

$$\frac{\langle \sum_n r_n \rangle}{\eta \sum_n s_n} \approx 1 - \kappa A + \kappa^2 B, \quad (\text{C.2})$$

where

$$\begin{aligned} A &= \frac{S_2}{S_1} \frac{1+\eta}{2} + w, \\ B &= \frac{S_3}{S_1} \left(\frac{1}{6} + \frac{\eta}{2} + \frac{\eta^2}{3} \right) + \frac{S_2}{S_1} w \left(\frac{1}{2} + \eta \right) + \frac{w^2}{2} \end{aligned}$$

with sums $S_p = \sum_n s_n^p$ ($p = 1, 2, 3$). Let us at first ignore the last, quadratic term in (C.2). The method of moments then suggests to estimate κ as

$$\hat{\kappa}_1 = A^{-1} \left(1 - \frac{\sum_n r_n}{\eta \sum_n s_n} \right).$$

The downward bias of this estimate can be corrected to some extent by taking account of the quadratic term in (C.2). Our final proposal for a direct estimate of κ (when η is known) is then

$$\hat{\kappa}_2 = \hat{\kappa}_1 + \frac{B}{A} \hat{\kappa}_1^2. \quad (\text{C.3})$$

The use of the approximate estimation method requires prior knowledge of the order of magnitude of κ : it should be used only if all times s_n and w are considerably smaller than κ^{-1} , so that the approximation (C.1) is applicable.

D Estimation of stochastic DKM parameters

Step 1 —Using the WLSQ procedure, as described in section 2.4.1, we find values of parameters $\hat{\kappa}$ and $\hat{\eta}$ that minimise the criterion

$$S \equiv S(\kappa, \eta) = \frac{1}{2} \sum_n \frac{(m_n - r_n)^2}{s_n}. \quad (\text{D.1})$$

These estimates are correctly centered. Their (approximate) dispersion matrix can be found using the ‘delta method’, i. e., by linearising the ‘estimation equations’ $DS(\hat{\kappa}, \hat{\eta}) = 0$, where the l. h. s. expression denotes the (column) vector of partial derivatives of S w. r. t. κ and η , evaluated at $(\hat{\kappa}, \hat{\eta})$. A first-order Taylor expansion of DS at the ‘true’ parameter (κ, η) yields the linear stochastic approximation

$$\begin{pmatrix} \hat{\kappa} \\ \hat{\eta} \end{pmatrix} \approx \begin{pmatrix} \kappa \\ \eta \end{pmatrix} - \mathbf{H}^{-1} DS(\kappa, \eta), \quad (\text{D.2})$$

where $\mathbf{H} \equiv \langle D^2 S(\kappa, \eta) \rangle$ denotes the expectancy of the matrix of second partial derivatives of S at (κ, η) . Let $\mathbf{C} \equiv \text{Cov}(DS(\kappa, \eta))$ denote the the covariance matrix of the ‘scores vector’ $DS(\kappa, \eta)$. Then from (D.2) we obtain an approximation \mathbf{V} to the covariance matrix of $(\hat{\kappa}, \hat{\eta})$ as a product of three matrices,

$$\text{Cov} \begin{pmatrix} \hat{\kappa} \\ \hat{\eta} \end{pmatrix} \approx \mathbf{H}^{-1} \mathbf{C} \mathbf{H}^{-1} = \mathbf{V}. \quad (\text{D.3})$$

Explicit expressions for the vector $DS(\kappa, \eta)$ and the matrices \mathbf{H} and \mathbf{C} are given in (Ehm and Wackermann, 2004). The validity of eq. (D.3) is demonstrated by the results of a simulation study shown in Fig. 8. Note that $\hat{\kappa}$ and $\hat{\eta}$ are highly correlated.

Figure 8 about here.

Step 2 —Estimation of the remaining parameters by minimising the log-likelihood $L(\hat{\kappa}, \hat{\eta}, \gamma_2, \rho)$ w. r. t. γ_2 and ρ fails similarly as mentioned in the preceding paragraph. In particular, consistent estimation of the parameter ρ seems to be impossible in this way, but it is reasonable to expect *ex ante* that $\rho \approx 1$. For interpretation of experimental data, the signal-to-noise ratio γ_2 is more important.

Its magnitude can be roughly estimated as follows: Let $q_1 < \dots < q_K$ be a set of ‘trial’ values in the range of magnitude of the ‘true’ value of ρ . For each q_k ($k = 1, \dots, K$) we calculate an estimate $\hat{\gamma}_2(q_k)$ by minimising the function $L(\hat{\kappa}, \hat{\eta}, \gamma_2, q_k)$ w. r. t. γ_2 . A plot of estimates $\hat{\gamma}_2(q_k)$ against q_k then should indicate the likely range of the ‘true’ γ_2 -value. More details are given in (Ehm and Wackermann, 2004).

References

- Allan, L. G., 2002. Temporal memory, in: Da Silva, J. A., Matsushima, E. H., Ribeiro-Filho, N. P. (Eds.), *Fechner Day 2002*, International Society for Psychophysics, Rio de Janeiro, pp. 91–97.
- Aschoff, J., 1963. Comparative physiology: diurnal rhythms. *Ann. Rev. Physiol.* 25, 581–600.
- Aschoff, J., 1998. Human perception of short and long time intervals: its correlation with body temperature and the duration of wake time. *J. Biol. Rhythms* 13, 437–442.
- Atmanspacher, H., Filk, T., 2003. Discrimination and sequentialization of events in perception, in: Buccheri, R., Saniga, M., Stuckey, W. M. (Eds.), *The Nature of Time: Geometry, Physics and Perception*, Kluwer, Dordrecht, pp. 67–75.
- Balsam, P., 1984. Relative time in trace conditioning, in: Gibbon, J., Allan, L. (Eds.), *Timing and Time Perception*, *Annals N. Y. Acad. Sci.* 423, 211–227.
- Bindra, D., Waksberg, H., 1956. Methods and terminology in studies of time estimation. *Psychol. Bull.* 53, 155–159.
- Block, R. A., 1990. Models of psychological time, in: Block, R. A. (Ed.), *Cognitive Models of Psychological Time*, Lawrence Erlbaum, Hillsdale, pp. 1–35.
- Carrel, A., 1931. Physiological time. *Science* 74, 618–621.
- Church, R. M., 1984. Properties of the internal clock, in: Gibbon, J., Allan, L. (Eds.), *Timing and Time Perception*, *Annals N. Y. Acad. Sci.* 423, 566–582.
- Church, R. M., Broadbent, H. A., 1990. Alternative representations of time, number, and rate. *Cognition* 37, 55–81.
- Ehm, W., Wackermann, J., 2003. Analysis of a stochastic version of the ‘klepsydra’ model, in: Berglund, B., Borg, E. (Eds.), *Fechner Day 2003*, International Society for Psychophysics, Stockholm, pp. 59–64.
- Ehm, W., Wackermann, J., 2004. Estimating the parameters of the stochastic klepsydra model, in: Oliveira, A., Teixeira, M., Borges, G., Ferro M. (Eds.), *Fechner Day 2004*, International Society for Psychophysics, Coimbra, pp. 349–353.
- Eisler, A. D., 2003. The human sense of time: biological, cognitive and cultural considerations, in: Buccheri, R., Saniga, M., Stuckey, W. M. (Eds.), *The Nature of Time: Geometry, Physics and Perception*, Kluwer, Dordrecht, pp. 5–18.
- Eisler, H., 1975. Subjective duration and psychophysics. *Psychol. Rev.* 82, 429–450.
- Gerstner, W., Kistler, W. M., 2002. *Spiking Neuron Models: Single Neurons, Populations, Plasticity*, Cambridge University Press, Cambridge.
- Gibbon, J., Church, R. M., 1990. Representation of time. *Cognition* 37, 23–54.
- Goudriaan, J. C., 1921. Le rythme psychique dans ses rapports avec les fréquences cardiaques et respiratoires. *Arch. Néerl. de Physiol.* 6, 77–110.
- Grondin, S., 2001. From physical time to the first and second moments of psychological time. *Psychol. Bull.* 127, 22–44.
- Hellström, Å., 1998. Net flow of mental content: possible basis for speed of time and subjective duration, in: Grondin, S., Lacouture, Y. (Eds.), *Fechner Day 98*, International Society for Psychophysics, Québec, pp. 243–248.
- Hellström, Å., 2003. Comparison is not just subtraction: effects of time- and space-order on subjective stimulus difference. *Percept. Psychophys.* 65, 1161–1177.
- Hoagland, H., 1933. The physiological control of judgments of duration: evidence for a chemical clock. *J. Gen. Psychol.* 9, 267–287.

- Holubář, J., 1969. *The Sense of Time. An Electrophysiological Study of Its Mechanisms in Man*, MIT Press, Cambridge (MA).
- Huygens, Ch., 1673. *Horologium oscillatorium, sive de motu pendulorum ad horologia aptato demonstrationes geometricae*, Muguet, Paris.
- James, W., 1890. *Principles of Psychology* (2 vols.), Holt, New York. [Unabridged edition in one volume, Dover, New York, 1950.]
- Janich, P., 1980. *Die Protophysik der Zeit. Konstruktive Begründung und Geschichte der Zeitmessung*, Suhrkamp, Frankfurt.
- Kandel, E. R., Schwartz, J. H., Jessell, T. M., 2000. *Principles of Neural Science* (4th ed.), McGraw-Hill, New York.
- Karatzas, I., Shreve, S. E., 1991. *Brownian Motion and Stochastic Calculus*, (2nd ed.), Springer, New York.
- Koch, G., Oliveri, M., Carlesimo, G. A., Caltagirone, C., 2002. Selective deficit of time perception in a patient with right prefrontal cortex lesion. *Neurology* 59, 1658–1659.
- Koch, G., Oliveri, M., Torriero, S., Caltagirone, C., 2003. Underestimation of time perception after repetitive transcranial magnetic stimulation. *Neurology* 60, 1844–1846.
- Linkenkaer-Hansen, K., Nikouline, V. V., Palva, J. M., Ilmoniemi, R. J., 2001. Long-range temporal correlations and scaling behavior in human brain oscillations. *J. Neurosci.* 21: 1370–1377.
- Ornstein, R. E., 1969. *On the Experience of Time*. Penguin, Harmondsworth.
- Oyama, T., 1978. Figural aftereffects, in: Held, R., Leibowitz, H. W., Teuber, H. L. (Eds.), *Handbook of Sensory Physiology. Vol 8: Perception*, Springer, Berlin, pp. 569–592.
- Pavlov, I. P., 1927. *Conditioned Reflexes*. Dover, New York.
- Pfaff, D., 1968. Effects of temperature and time of day on time judgments. *J. Exp. Psychol.* 76, 419–422.
- Pöppel, E., Giedke, H., 1970. Diurnal variation of time perception. *Psychol. Forsch.* 34, 182–198.
- Pöppel, E., 1972. Oscillations as possible basis for time perception, in: Fraser, J. T., Haber, F. C., Müller, G. H. (Eds.), *The Study of Time*, Springer, Berlin, pp. 219–241.
- Pöppel, E. (1978) Time perception, in: Held, R., Leibowitz, H. W., Teuber, H. L. (Eds.), *Handbook of Sensory Physiology. Vol. 8: Perception*, Springer, Berlin, pp. 713–729.
- Pouthas, V., Perbal, S., 2004. Time perception depends on accurate clock mechanisms as well as unimpaired attention and memory processes. *Acta Neurobiol. Exp.* 64, 367–385.
- Rammsayer, T. H., 1990. Temporal discrimination in schizophrenic and affective disorders: evidence for a dopamine-dependent internal clock. *Int. J. Neurosci.* 53, 111–120.
- Rammsayer, T., Vogel, W. H., 1992. Pharmacological properties of the internal clock underlying time perception in humans. *Neuropsychobiology* 26, 71–80.
- Reichenbach, H., 1957. *The Philosophy of Space and Time*, Dover, New York.
- Richelle, M., Lejeune, H., 1984. Timing competence and timing performance: a cross-species approach, in: Gibbon, J., Allan, L. (Eds.), *Timing and Time Perception*, *Annals N. Y. Acad. Sci.* 423, 254–268.
- Rubia, K., Smith, A., 2004. The neural correlates of cognitive time management: a review. *Acta Neurobiol. Exp.* 64, 329–340.
- Scheving, L. E., Halberg, F., Pauly, J. E., 1974. *Chronobiology*, Thieme, Stuttgart.
- von Steinbüchel, N., Wittmann, M., Szlag, E., 1999. Temporal constraints of perceiving, generating, and integrating information: clinical indications. *Restor. Neurol. Neurosci.* 14, 167–182.

- Treisman, M., 1963. Temporal discrimination and the indifference interval: Implications for a model of the 'internal clock'. *Psychol. Monogr.* 77, whole No 576.
- Treisman, M., 1984. Temporal rhythms and cerebral rhythms, in: Gibbon, J., Allan, L. (Eds.), *Timing and Time Perception*, *Annals N. Y. Acad. Sci.* 423, 542–565.
- Treisman, M., Faulkner, A., Naish, P. L. N., Brogan, D., 1990. The internal clock: evidence for a temporal oscillator underlying time perception with some estimates of its characteristic frequency. *Perception* 19, 705–748.
- Tuckwell, H. C., 1988. *Introduction to Theoretical Neurobiology* (2 vols.), Cambridge University Press, Cambridge.
- Uhlenbeck, G. E., Ornstein, L. S., 1935. On the theory of Brownian motion. *Phys. Rev.* 36, 823–841.
- Usher, M., McClelland, J. L., 2001. The time course of perceptual choice: the leaky, competing accumulator model. *Psychol. Rev.* 108, 550–592.
- Wackermann, J., Miener, M., 2002. Reproduction of time intervals under photic driving of the brain's electrical activity, in: Da Silva, J. A., Matsushima, E. H., Ribeiro-Filho, N. P. (Eds.), *Fechner Day 2002*, International Society for Psychophysics, Rio de Janeiro, pp. 558–563.
- Wackermann, J., Pütz, P., Büchi, S., Strauch, I., Lehmann, D., 2002. Brain electrical activity and subjective experience during altered states of consciousness: ganzfeld and hypnagogic states. *Int. J. Psychophysiol.* 46, 123–146.
- Wackermann, J., Ehm, W., Späti, J., 2003. The 'klepsydra model' of internal time representation, in: Berglund, B., Borg, E. (Eds.), *Fechner Day 2003*, International Society for Psychophysics, Stockholm, pp. 331–336.
- Wackermann, J., 2004. From neural mechanics to the measure of subjective time: the klepsydra model, in: Oliveira, A., Teixeira, M., Borges, G., Ferro M. (Eds.), *Fechner Day 2004*, International Society for Psychophysics, Coimbra, pp. 164–169.
- Wackermann, J., 2005. Experience of time passage: phenomenology, psychophysics, and biophysical modelling, in: Buccheri, R., Saniga, M., Elitzur, A. (Eds.), *Endophysics, Time, Quantum and the Subjective*, World Scientific, Singapore, in press.
- Wearden, J. H., Ferrara, A., 1993. Subjective shortening in human's memory for stimulus duration. *Quart. J. Exp. Psychol.* 46B, 163–186.
- Wearden J. H., Penton-Voak, I. S., 1995. Feeling the heat: body temperature and the rate of subjective time, revisited. *Quart. J. Exp. Psychol.* 48B, 129–141.
- Wearden, J. H., 2004. Decision processes in models of timing. *Acta Neurobiol. Exp.* 64, 303–317.
- White, C. T., 1963. Temporal numerosity and the psychological unit of duration. *Psychol. Monogr.* 77, 1–37.
- Whittrow, G. J., 1988. *Time in History*, Oxford University Press, Oxford.
- Winfree, A. T., 1980. *The Geometry of Biological Time*, Springer, Berlin.
- Wing, A. M., Kristofferson, A. B., 1973. Response delays and the timing of discrete motor responses. *Percept. Psychophys.* 14, 5–12.
- Woodrow, H., 1930. The reproduction of temporal intervals. *J. Exp. Psychol.* 13, 473–499.
- Woodrow, H., 1951. Time perception, in: Stevens, S. S. (Ed.), *Handbook of Experimental Psychology*, Wiley, New York, pp. 1224–1236.
- Zakay, D., Block, R. A., 1997. Temporal cognition. *Curr. Direct. Psychol. Sci.* 6, 12–15.

List of abbreviations

DKM	dual klepsydra model
EEG	electroencephalogram
ICM	internal clock model
ISI	inter-stimulus interval
IOS	inflow/outflow system
KRD	klepsydra reproduction distribution
KRF	klepsydra reproduction function
SDKM	stochastic dual klepsydra model
TOE	time order error
TPT	time production task
TRC	time reproduction curve
TRT	time reproduction task
WLSQ	weighted least squares

Figure legends

Fig. 1. The internal clock model. — P = pacemaker; S = switch; E = external event controlling the switch; A = pulse count accumulator; M_w = working memory register; M_r = long-term reference memory; C = comparator. Freely adapted from Church (1984).

Fig. 2. Experimental time reproduction curves, showing average reproduced times r (lower graphics), and average reproduced/presented times ratios (upper panel) as functions of presented stimulus durations s . —Left (a): Data from a study by Wackermann and Miener (2002). Right (b): Data reported by A. Eisler (2003); filled circles: Swedish population; open circles: African population.

Fig. 3. Examples of inflow/outflow systems. —Left (a): hydrodynamic IOS ('klepsydra'); right (b): electrical RC -circuit with outflow coefficient $\kappa = (RC)^{-1}$.

Fig. 4. Dual klepsydra model (DKM) of time reproduction. —Top: Klepsydra 1 is filled from $t = 0$ to $t = s$ (stimulus duration) and leaks for $t > s$. Klepsydra 2 is filled from $t = s + w$ on, until states of both klepsydrae become equal (reproduction). Bottom: DKM with stochastic inflows. Shown are two sample trajectories for the same stimulus duration s , resulting in different reproduced times R_1, R_2 .

Fig. 5. Klepsydra reproduction functions (KRF). —Left (a): Theoretical KRF's for fixed $\eta_* = 1$ and varied values of the parameter $\kappa \in \{0, .001, .002, .005, .01, .02\}$. Increasing curvatures of the KRF's correspond to higher κ 's. Right (b): KRF's fitted to experimental data (cf. Figs. 2a,b).

Fig. 6. Reproduction of a bipartitioned time interval. —Top (a): Reproduction of the entire duration s . Bottom (b): Serial reproduction of partial durations t_1, t_2 . —The semicircular dashed arcs lead from the beginning of the original time interval to the beginning of the reproduced interval; the vertical arrowhead indicates the subject's 'now' at the start of the reproduction.

Fig. 7. Cumulative reproduction functions \mathcal{T} (bottom) and their derivatives $\rho \equiv d\mathcal{T}/dt$ (top) for reproductions of durations $s = 30$ and 60 s, with $\kappa = 0.015 \text{ s}^{-1}$. Continuous increase of the density functions $\rho(t)$ with progressing time t indicates subjective 'speeding up' of time passage.

Fig. 8. Scatterplot of 200 pairs of WLSQ estimates. Each pair $(\hat{\kappa}, \hat{\eta})$ was calculated from $N = 80$ triples (s_n, w_n, r_n) . Durations s_n were varied at 8 levels, from 2 to 22.6 s. The ISI was constant, $w_n = 5$ s for all n . Reproduced times r_n were simulated according to the SDKM under parameters $\kappa = 0.02$, $\eta = 1$, $\rho = 1$, $\gamma_2 = 3$. Dispersion ellipsoid was determined by covariance matrix \mathbf{V} , scaled so as to contain nominally 90% of the pairs.

Figures

Fig. 1

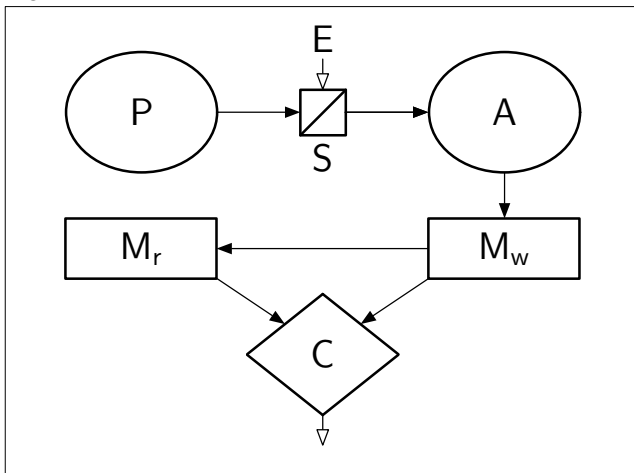


Fig. 2

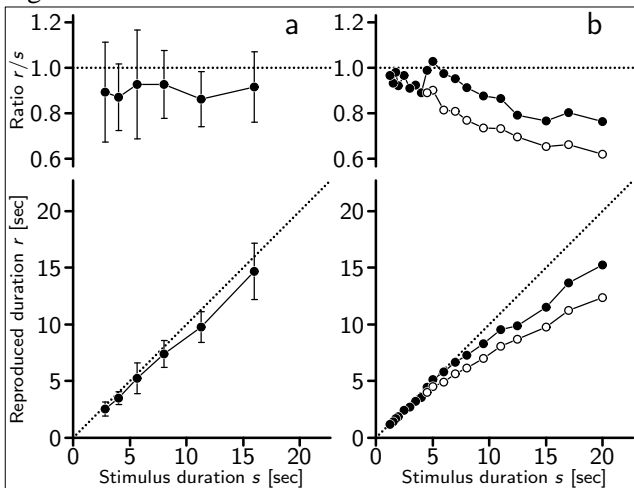


Fig. 3

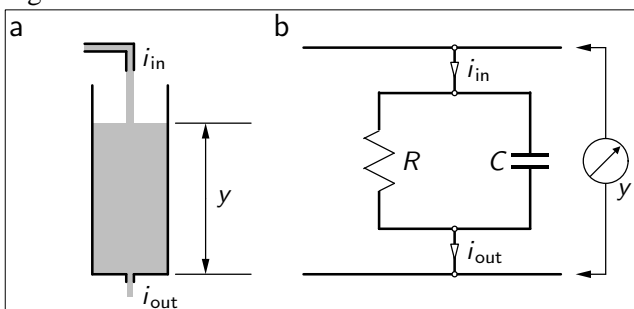


Fig. 4

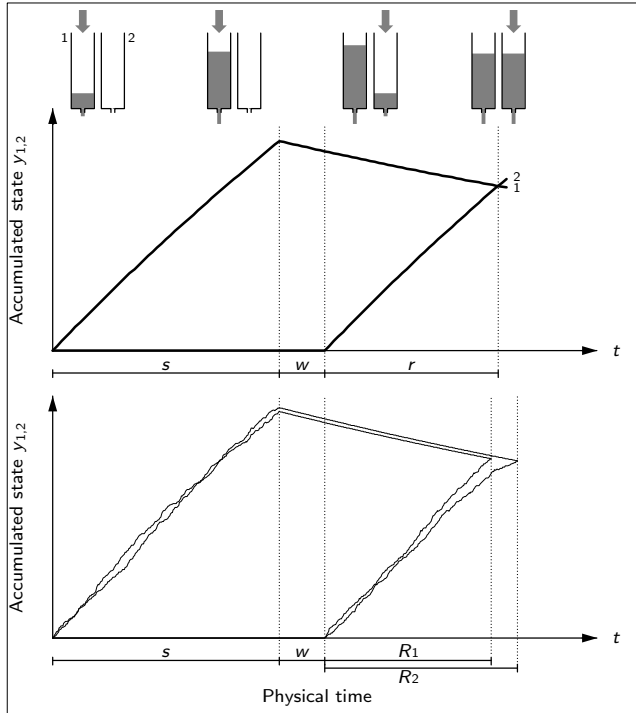


Fig. 5

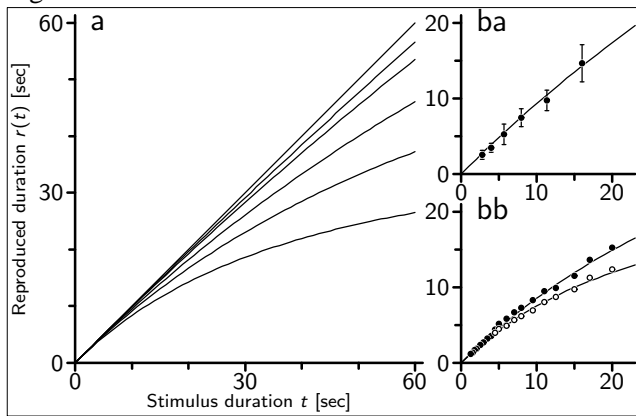


Fig. 6

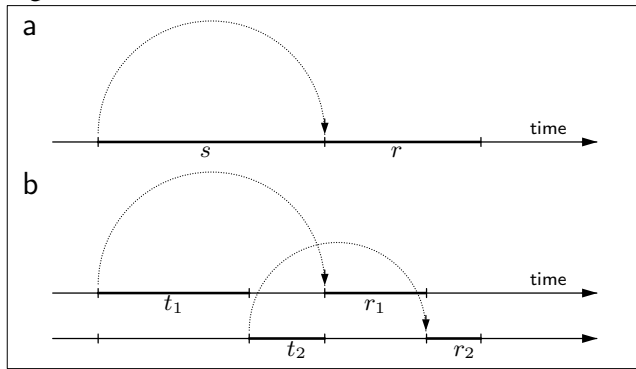


Fig. 7

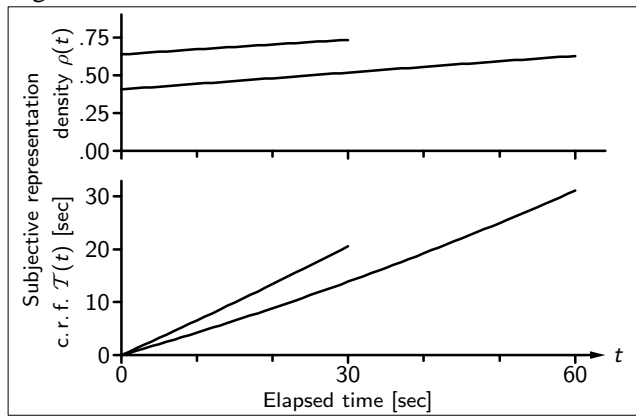


Fig. 8

